Carbohydrate Polymers 121 (2015) 468–476

Contents lists available at ScienceDirect

Carbohydrate Polymers

journal homepage: www.elsevier.com/locate/carbpol

Plasma modified nanofibres based on gum kondagogu and their use for collection of nanoparticulate silver, gold and platinum

Vinod Vellora Thekkae Padil, Martin Stuchlík, Miroslav Černík*

Department of Nanomaterials in Natural Sciences, Institute for Nanomaterials, Advanced Technologies and Innovation, Technical University of Liberec, Studentská 1402/2, 460 08 Liberec, Czech Republic

ARTICLE INFO

Article history:
Received 28 October 2014
Received in revised form
28 November 2014
Accepted 29 November 2014
Available online 31 December 2014

Keywords:
Gum kondagogu
Polyvinyl alcohol
Electrospun nanofibres
Plasma treatment
Nanoparticle removal

ABSTRACT

Electrospun nanofibre membranes from blend solutions of deacetylated gum kondagogu and polyvinyl alcohol of various weight proportions were prepared. The electrospun membrane was cross linked by heating at 150 °C for 6 h and later modified by methane plasma treatment. Membranes were successively used for the removal of nanoparticles (Ag, Au and Pt) from water. Pt nanoparticles with the smallest size (2.4 ± 0.7 nm) has a higher adsorption capacity (270.4 mg/g and 327.2 mg/g) compared to Au and Ag nanoparticles with particle sizes 7.8 ± 2.3 nm and 10.5 ± 3.5 nm onto nanofibre membrane (NFM) and methane plasma treated membrane (P-NFM). The extraction efficiency of P-NFM for the removal of nanoparticles in water is higher compared to untreated membranes. The adsorption kinetics were evaluated by pseudo-first order and pseudo-second order models for the extraction of nanoparticles from water, with the pseudo-second order model providing a better fit. The reusability and regeneration of the P-NFM for consecutive adsorption was also established.

1. Introduction

The widespread use of metal nanoparticles in pharmaceutical, medical, food and cosmetic industries represents a potential source of pollution, which may lead to serious health problems in the near future. Micropollutants are emerging contaminants in drinking water and a challenging task is to discover novel technologies for their removal from the environment. Various technologies currently available for removal of environmental contaminants are based on processes such as oxidation, precipitation, activated carbon adsorption, coagulation/co-precipitation, ion-exchange and different types of membrane filtration (microfiltration, ultrafiltration, nanofiltration, reverse osmosis, membrane distillation and electro dialysis) (Luo, Guo, Ngo, Nghiem, & Hai, 2014; Suarez, Lema, & Omil, 2009; Choi, Kim, & Kim, 2008; Kovalova et al., 2013; Garcia, Moreno, Cartmell, Rodriguez-Roda, & Judd, 2013; Yangali-Quintanilla et al., 2011; Radjenovic, Petrovic, & Barcelo, 2009). In all of these technologies, the removal of nanoparticles is highly dependent on the physico-chemical properties of the micropollutants and the treatment conditions (Schafer, Nghiem, & Semiao, 2011). Furthermore, several membrane systems incur higher capital or operational costs than conventional water treatment technologies. Green technology based on various natural adsorbents is known to be effective in solving environmental tasks of contaminated water treatment. Electrospun nanofibre membranes are potential candidates for the removal of nanoparticles from aqueous solutions. Compared to powder materials, they have a higher surface area, smaller pore size, higher permeability and the potential functionality of active groups at a nanoscale (Li, Yue, Jing, Bai, & Dai, 2011). Recently, surface modified electrospun nanofibres or nanocomposites based on natural and synthetic polymers such as PVA, gum Ghatti, Fe_3O_4 nanocomposites, poly(acrylo-amidino ethylene amine), and polyacrylonitile/polypyrrole core-shells, etc. have been used for the removal of nanoparticles and toxic metals from water (Desai et al., 2009; Mahanta & Valiyaveettil, 2011; Qureshi, DSouza, Mallampati, & Valiyaveettil, 2014).

The removal of nanoparticles from water using electrospun membranes based on plant polysaccharide is a new approach. Natural plant derived gums, which are important forest products, have potential value as food additives, emulsifiers, pharmaceutical ingredients, and are used as biosorbents for the removal of environmental contaminants (Verbeken, Dierckx, & Dewettinck, 2003; Phillips & Williams, 2001; Vinod et al., 2009; Vinod, Sashidhar, & Sukumar, 2010). Each gum has its own unique properties and applications. The morphological, physical, chemical, structural, rheological, pharmaceutical and emulsifying properties of gum kondagogu (GK) have been established (Vinod et al., 2008a; Vinod, Sashidhar, Sarma, & Vijay Saradhi, 2008b; Naidu et al., 2009a;

* Corresponding author. Tel.: +420 734872403.
E-mail address: miroslav.cernik@tul.cz (M. Černík).

http://dx.doi.org/10.1016/j.carbpol.2014.11.074
0144-8617/

Naidu et al., 2009b). Compared to the other gums, GK has high volatile acidity and water-binding (hydrogel) properties.

Electrospinning is a fabrication technique which is applied to various polymeric materials to produce membranes for potential applications in the field of medicine, drug delivery, tissue engineering, wound healing and water filtration (Still & Von Recum, 2008; Thanasi, Singh, & Ramakrishna, 2008). The spinnability of polymers under an electrical field is a crucial parameter for their applicability in various fields. Electrospinning of polymers and obtaining uniform nanofibres depends on many factors including the molecular weight, degree of deacetylation, purity, solubility, charged group distribution, gelling behaviour, molecular weight distribution and architecture (branched, linear etc.) of the polymers. Other factors include their solution properties (viscosity, surface tension, chain entanglement and electrical conductivity) as well as process parameters (electric potential, flow rate and concentration, distance between the capillary and collection screen, ambient temperature, humidity and air velocity in the chamber) (Frenot & Chronakis, 2003; Wilkes, 2001). So far, electrospinning of natural tree based gums such as gum Arabic, gum Tragacanth, gum karaya and GK has not been attempted. The high molecular weight, viscosity and polyonionic behaviour of tree-based polymers has prevented the formation of fibres during electrospinning.

Blending of these polymers with synthetic polymers such as polyvinyl alcohol and poly(ethylene oxide) improves the solubility of the polymer and hence the spinability for electrospinning (Toskas et al., 2011). The nanofibres are cross-linked by heating the NFM at 150 °C for 6 h and later by methane plasma treatment. Water resistant NFM are obtained by thermal cross-linking and plasma treatment. It has been reported that chitosan/PEO nanofibres and polyethyleneimine/PVA nanofibres produced by electrospinning were cross-linked via heat treatment (Muzzarelli, EI Mehtedi, & Mattioli-Belmonte, 2014; Fang et al., 2011). Recently, nanofibres have been produced from gum Tragacanth blended with PVA solutions at different ratios using the electrospinning technique (Ranjbar-Mohammadi, Bahrami, & Joghataei, 2013).

The extraction efficiency of the electrospun membranes for the removal of nanoparticles from water can be improved by plasma treatment to improve their hydrophobic character, (Svirachev & Tabaliov, 2005; Guo et al., 2010). Plasma treatment is considered a versatile and effective method for modifying the surface properties of polymeric materials or introducing the desired chemical groups onto the surface of the electrospun membranes without affecting their bulk properties (Wang, Ding, Yu, & Wang, 2011).

In the present study, PVA was blended with deacetylated gum kondagogu (DGK) and from the blend solutions of different weight ratios a nanofibre membrane (NFM) was produced using electrospinning. The optimum blend ratios of PVA and DGK and electrospinning parameters and their influence on membrane morphology were studied. The NFM was cross-linked via heat treatment and later by surface modification by methane plasma. The adsorption capacities and extraction efficiencies for the removal of nanoparticles were evaluated. Membrane morphology and other characteristics were analysed using scanning electron microscopy, transmission electron microscopy, UV–vis and ATR-FTIR techniques. Pseudo-first order and pseudo-second order kinetic models were used to evaluate the mechanism of adsorption of the NPs onto NFM.

2. Experimental

2.1. Materials

Gum kondagogu (GK) samples were collected from the Girijan Co-operative Corporation, Hyderabad, India. Polyvinyl alcohol, *Mw* 88,000, degree of 88%, $AgNO_3$, $HAuCl_4{\cdot}3H_2O$, H_2PtCl_6, and NH_4OH were purchased from Sigma-Aldrich, USA. De-ionized water was used in all of the experiments.

2.2. Preparation of deacetylated GK and its parameters

GK was powdered in a high-speed mechanical blender and later sieved using a bin (mesh size—250 μm), so as to obtain fine and uniform samples. The DGK was prepared as per the reported method (Vinod & Sashidhar, 2009). In brief, GK powder (1 g) was accurately weighed and dispensed into clean glass beakers containing one litre of deionized water. The gum solutions were placed on magnetic stirrer at room temperature and gently stirred overnight after which they were allowed to stand at room temperature for 12 h, so as to separate out any un-dissolved matter. The resulting gum solutions were subsequently centrifuged to obtain clear solutions. Three volumes of each of the gum solution were mixed with one volume of 1 M NaOH. After incubation for 6 h at room temperature with gentle agitation on a magnetic stirrer, one volume of 1 M HCl was added to neutralize the solution (to a final pH of 7.0). The resulting DGK solution was dialysed (dialysis tubing DTV 12000.09.000; *Mw* range; 12–14 kDa, Medicell International Ltd., London) extensively against deionized water to remove any residual salts. The gum solution was then centrifuged and the clear solutions so obtained were freeze-dried and stored until further use. The deacetylation was monitored by FTIR analysis.

The molecular mass distribution of the DGK was determined using the technique of gel permeation chromatography (GPC) linked to multi angle laser light scattering (MALLS). $NaNO_3$ (0.1 M) containing 0.005% sodium azide (biocide) was used as the eluent and the solution was filtered using a GSWP 0.45 μm filter (Millipore) and degassed by means of a vacuum degasser (CS615/Cambridge Scientific Instruments) before use. The sample of DGK (0.2 wt%) was prepared in 0.1 M $NaNO_3$ solution and left overnight on a roller to complete the dissolution. The GPC system consisted of a Suprema column with the following specifications [dimensions: 300 mm × 8 mm; bead size: 10 μm and pore size: 100 Å]. The column was protected by a guard column (Polymer Standards Service GmbH)]. The flow rate was set to 0.5 mL/min. using a Waters Corporation HPLC pump in conjunction with a Rheodyne 7125 model injection system (loop volume 200 μL). A Dawn DSP Laser Photometer and OPTILAB DSP Interferometric Refractometer (Wyatt Technology Corporation) were used as detectors. The gum samples were filtered through 0.45 μm syringe filters before being injected into the HPLC column. All measurements were performed in triplicate. The molecular mass distributions and rms radius moments of the gum were determined using the designated Astra software for Windows (4.90.08, QELSS 2. XX). The data was fitted using the first-order polynomial and Zimm method. The refractive index increment (dn/dc) value for DGK was determined to be 0.140 mL/g (Vinod et al., 2008a).

2.3. Preparation of the PVA/DGK blend solution and electrospinning

An aqueous solution of PVA (10 wt%) was prepared by adding PVA to de-ionized water and heating at 90 °C in a magnetic stirrer for 5 h. The PVA solution was then mixed with DGK solutions (5 wt%) in different weight ratios of PVA/DGK (100/0, 50/50, 60/40, 70/30, 80/20, 90/10 and 0/100) and kept in the magnetic stirrer for another 5 h to ensure complete mixing. All of the solutions were then centrifuged to remove suspended particles before electrospinning.

A Fungilab viscometer (ALPHA R series, Barcelona, Spain) and Tesiometer (K6, KRUSS GmbH, Hamburg, Germany) were used to measure the viscosity and surface tension of the blended solution,

respectively. The pH and conductivity of the electrospinning solution were determined using a Multi 3430 Digital pH/conductivity meter (WTW GmbH, Weiheim, Germany). All of the measurements were performed at 25 °C. The measurements were done in triplicate and the values reported as mean ± S.D.

The electrospinning was carried out using a nanospider electrospinning machine (NS IWS500U, Elmarco, Czech Republic) under the following conditions: spinning electrode width = 500 mm, effective nanofibre layer width = 200–500 mm; spinning distance = 130–280 mm, substrate speed = 0.015–1.95 m/min, process air flow = 20–150 m^3/h, and voltage 0–50 kV. The surface area of the produced PVA/DGK membranes was analysed using the Brunauer–Emmett–Teller (BET) technique (Autosorb iQ, Quantachrome, Florida, USA). The nanofibre shape and NFM surface morphologies were investigated using a scanning electron microscope (SEM ZEISS, Ultra/Plus, Germany).

2.4. Methane plasma treatment and cross-linking

The methane plasma treated membrane (P-NFM) was produced by treating the NFM membrane in a radio frequency plasma reactor (BalTec Maschinenbau AG, Pfäffikon, Switzerland). The plasma chamber was thoroughly purged with a continuous flow of the gas used during the treatment to reduce trace amounts of air and moisture. During the treatment, the gas flow was adjusted in order to keep a constant pressure of 0.2 mbar inside the chamber. The duration of the treatment was varied from 2 min to 5 min. The plasma conditions and process parameters were (power 20 W; voltage 300 V; time 5 min.; pressure 20 Pa; plasma gas purity 99.997%; electrode area 48 cm^2; inter-electrode distance 50 mm and chamber volume 1000 cm^3).

The membranes were cross-linked by keeping the membrane in an oven at 150 °C for 1 h to 6 h. The initial and final weight of the NFM was determined before and after heat treatment to determine any loss in weight of the fibre during the heating process. The surface wettability was determined by measuring the water contact angle (θ) using the sessile drop method with OCA20 equipment (Data Physics, Germany) and SCA-20 software. The presented data are the average of the three measurements. The stability of the P-NFM (10 mg) in neural, acidic and basic conditions was tested for its sustainability by soaking for 5 days in water, 0.5 N HCl and 0.5 N NaOH, respectively. The degree of stability (DS) was determined using the following equation:

$$\mathrm{DS}\,(\%) = \frac{W_2}{W_1} \times 100 \tag{1}$$

where W_1 and W_2 are the weights of the dried fibre membranes before and after the experiment, respectively.

2.5. Preparation of GK stabilised nanoparticles (Au, Ag and Pt)

Au, Ag and Pt nanoparticles were synthesized using the corresponding Au, Ag and Pt salts ($AgNO_3$, $HAuCl_4{\cdot}3H_2O$ and H_2PtCl_6) with GK acting as the reducing and stabilizing agent (Vinod, Saravanan, Sreedhar, Keerthi Devi, & Sashidhar, 2011). In a typical preparation 100 μL of salt solution (5×10^{-3} M) was added to 10 mL of GK aqueous solution (100 mg GK) in a separate 100 mL conical flask. The pH of the colloidal solution was maintained by adding 0.1 N HCl or 0.1 N NaOH. For the synthesis of Ag and Au nanoparticles, the solution was kept agitated in an orbital shaker (Innova' 43, New Brunswick Scientific Co. Ltd., NJ, USA) at 65 °C (Ag) and 75 °C (Au) at 250 rpm for 1 h. The colour of the solution turned light yellow (Ag) or wine red (Au) after 1 h indicating the formation of nanoparticles. Pt nanoparticles were synthesized by autoclaving the solution at 15 psi for 15 min and the solution turned a dark colour, indicating the formation of Pt nanoparticles. The formation of Ag, Au and Pt nanoparticles was also confirmed by UV–vis spectroscopic measurements.

Nanoparticle size distributions were determined using a transmission electron microscope (TEM; Tecnai F30, Japan; acceleration voltage 15 kV). For TEM measurements, samples were prepared by dropping 10–20 μL of nanoparticle dispersions onto a copper grid and subsequently drying at room temperature after removing the excess solution using filter paper.

2.6. Adsorption study

To determine the adsorption efficiency, 10 mg each of P-NFM and NFM were added to 100 mL of nanopartiicle solution of a known concentration (2×10^{-4} M). The whole mixture was agitated (200 rpm) at room temperature for 180 min and aliquots were collected and nanoparticle concentrations were determined using ICP–MS (NexION 300 Q, PerkinElmer, USA).

A kinetic adsorption study was conducted under the same conditions but the samples were collected at a different time. The adsorption efficiency and the adsorption capacity were calculated using standard equations (Eqs. (2) and (3)).

$$\text{Adsorption efficiency}\,(\%\mathrm{AE}) = \frac{A_0 - A_f}{A_0} \times 100 \tag{2}$$

$$\text{Adsorption capacity}\,(Q_e) = \frac{\left(A_0 - A_f\right)}{m} \times V \tag{3}$$

where in Eqs. (2) and (3), A_0 and A_f represents the initial and final concentrations (mg/L) of nanoparticles in solution, m is the mass of the NFM (g) and V is the volume of the solution (L). The adsorption and experiments were done in triplicates and all of the results are presented as mean ± S.D.

The surface morphologies of the NFM before and after nanoparticle extraction were investigated using a scanning electron microscope (ZEISS, Ultra/Plus, Germany). EDX analysis of the NFM was also carried out to establish whether the corresponding metal ions were present in the nanofibre membrane after adsorption of the various nanoparticles.

FTIR spectra were recorded in the range of 400–4000 cm^{-1} using a NICOLET IZ10 module (Thermo scientific, USA). The samples were analysed directly on an attenuated total reflection (ATR) platform. The spectrometer is equipped with a multi-reflection variable angle horizontal ATR accessory. Measurements were performed on P-NFM and NFM with adsorbed nanoparticles. All of the spectra were baseline corrected by automatic software control and were normalized thereafter.

The kinetic adsorption study of P-NFM was performed by agitating 10 mg of NFM with various concentrations of nanoparticle (Ag, Au and Pt) in water at 25 °C. The samples were taken at each time interval and the initial and final concentrations of nanoparticle were calculated using the following equation:

$$\text{adsorption capacity}\,(Q_t) = \frac{A_0 - A_t}{m} \times V \tag{4}$$

where Q_t is the adsorption capacity at time t, A_0 is the initial concentration and A_t is the final concentration of NP at time t, respectively, m is the weight (g) of NFM, and V is the volume of the experimental solution (L).

To evaluate the suitability and practical applications of NFM for water treatment, it was subjected to consecutive adsorption and desorption cycles. Desorption studies of the adsorbed nanoparticle (Ag, Au and Pt) were carried out by agitating the P-NFM (10 mg) in 0.2 N HCl for a period of 6 h. The initial and final concentrations of nanoparticle were determined using ICP-MS. The sorbent sample was regenerated and reused and the adsorbent was tested for its reusability for five cycles of operation.

3. Results and discussion

3.1. Determination of DGK molecular mass distribution

The molecular mass distribution of DGK determined by GPC/MALS was fitted with a first-order polynomial using the Zimm method. The determined average molecular mass of 1.14×10^6 g/mol is higher compared to the molecular mass of gum Arabic (6.2×10^5 g/mol) and lower compared to gum karaya (16×10^6 g/mol) reported in the literature (Mahendran, Williams, Phillips, Al-Assaf, & Baldwin, 2008; Le-Cerf, Irinei, & Muller, 1990). Details of the molecular mass distribution determined by GPS/MALLS are attached (Supporting information 1).

3.2. Effect of various parameters to electrospinning

The viscosity, surface tension, conductivity and pH of various weight ratios of PVA/DGK blends (100/0, 90/10, 80/20, 70/30, 60/40, 50/50, 40/60 and 0/100) are presented in Table 1 and the corresponding electrospun nanofibres are shown in Fig. 1.

Electrospinning of DGK alone (PVA/DGK ratio of 0/100) was unsuccessful due to the high viscosity of the DGK solution and resulted in the formation of droplets and no fibres. The addition of PVA in different proportions resulted in fibres with a different morphology and diameter. The smallest addition (ratios 40/60, 50/50 and 60/40) facilitates nanofibre formation but the fibres are not smooth or uniform and contain impurities. This may be due to the high viscosity of the blend solution which requires a higher voltage, which in turn leads to poor morphology, irregular fibre diameter, and increases the chance of bead formation (Homayoni, Ravandi, & Valizadeh, 2009).

Increasing the amount of PVA leads to the formation of uniformly-sized nanofibres. SEM images of PVA/DGK nanofibres produced from solutions with a ratio of 70/30 and higher have a uniform diameter and morphology.

The viscosity and surface tension of the solution are the two main parameters influencing the electrospinning (Lee, Kim, Bang, Jung, & Lee, 2003; Kim, Kim, Jin, & Chin, 2005). Table 1 shows that by increasing the amount of PVA in the PVA/DGK blend, the viscosity decreases. For the weight ratio of (70/30; PVA/DGK), where uniform nanofibres are formed, the viscosity is 5400 mPa s.

However, the viscosity is not the only reason for better spinability of blended solutions. The —OH groups present in the PVA interact with the —COO and —OH groups of the DGK to form hydrogen bonds, confirmed by FTIR (Fig. 4A). It has been reported in the case of *Ulva Rigida* polymers, that the addition of PVA reduces the viscosity of the blend solution and intercalates the hydrogen bonds forming between the polymer chains which helps to effectively produce uniform-sized nanofibre membranes (Toskas et al., 2011).

The produced nanofibres have a uniform diameter (e.g. 150 nm for the weight ratio of 70/30; PVA/DGK) and linear structure. The digital photographs of NFM (untreated) and P-NFM (methane plasma treated membrane) are presented in Fig. 2b and d. SEM pictures, for the untreated sample (Fig. 2a), the smooth surface of the NFM is clearly observed, whereas the P-NFM were notably roughened by the methane plasma treatments, as seen in Fig. 2c. Typically, plasma treatment modifies the surface by grafting hydroxyl (—OH), carbonyl (—C—O), and carboxylate (—COOH) groups (Svirachev & Tabaliov, 2005).

The spinning character of DGK is resolved through the application of NaOH treatment which hydrolyses GK polymer chains and reduces their molecular weight (Vinod et al., 2008b). Further deacetylation (monitored by FTIR analysis) of the gum results in the disappearance of the acetyl group (peak at 1726 cm^{-1} in the FTIR spectrum; Supporting information 2) increasing the solubility of the gum in water (Le Cerf et al., 1990).

Changes in morphology caused by the plasma treatment are confirmed by measuring the surface area. The BET surface area of NFM and P-NFM is 6.15 m^2/g and 9.79 m^2/g, respectively, which is a 60% growth rate. In our study the water contact angle of P-NFM increased dramatically to $130.5 \pm 0.5^\circ$, overtaking the NFM, which showed a lower water contact angle ($105.5 \pm 0.5^\circ$).

3.3. Stability of NFM

The stability of P-NFM was tested in aqueous, acidic and alkaline solutions. Fig. 3 shows the degree of stability (DS) of P-NFM calculated according to Eq. (1) in deionized water, 0.5 N HCl and 0.5 N NaOH, respectively. In the aqueous solution the DS decreased to 92.5% after 8 h and then become almost stable after 5 days of contact (a decrease to approximately 90%). The DS in 0.5N HCl reduced to 87% within 24 h of contact and then it became stable (decreasing to 85% after 5 days). The biggest decrease in DS was observed in 0.5 N NaOH. The DS of the P-NFM decreased rapidly to 87% within 8 h and then moderately to 78% after 5 days of contact.

3.4. Adsorption studies of nanoparticles (Au, Ag and Pt) on NFM

Synthesized Au, Ag and Pt nanoparticle were used to study their uptake by the produced membranes. The nanoparticle is characterized by a distinct colour which is shown and the nanoparticle has a different mean diameter, which was quantitatively determined by TEM analysis (Supporting information 3b–d). Pt nanoparticles are the smallest with a mean size of 2.4 ± 0.7 nm, and then Au nanoparticle of 7.8 ± 2.3 nm and Ag nanoparticle of 10.5 ± 3.5 nm are larger.

The UV–vis spectra of synthesized Au and Ag nanoparticle showed absorbance maxima at 525 nm and 412 nm, respectively (Supporting information 3e). The crystalline nature of Ag, Au, and Pt nanoparticle was confirmed by X-ray diffraction analysis (Supporting information 3f).

The major functional groups present in GK, DGK, PVA and P-NFM were assessed using ATR-FTIR spectroscopy (Fig. 4A). The peaks at 3350 cm^{-1}, 2925 and 2850 cm^{-1} were attributed to the

Table 1
Electrospinning parameters of PVA/DGK blend solutions in water at 25 °C.

Solution composition	Solution properties[#]			
PVA/DGK ratio	Viscosity (mPa s)	Surface tension (mN/m)	Conductivity (mS/cm)	pH
100/0	2400 ± 34	49.5 ± 0.1	1.0 ± 0.1	6.0
90/10	3570 ± 46	50.5 ± 0.1	1.35 ± 0.1	6.0
80/20	4100 ± 57	54.5 ± 0.1	1.68 ± 0.1	6.1
70/30	5400 ± 69	56.9 ± 0.1	2.05 ± 0.2	6.2
60/40	6200 ± 77	58.2 ± 0.1	2.56 ± 0.5	6.4
50/50	6800 ± 98	59.5 ± 0.2	3.05 ± 0.7	6.5
40/60	7000 ± 101	60.0 ± 0.2	3.18 ± 0.8	6.5
0/100	7500 ± 110	60.5 ± 0.2	3.57 ± 0.9	6.8

[#] Values = mean ± S.D (n = 3).

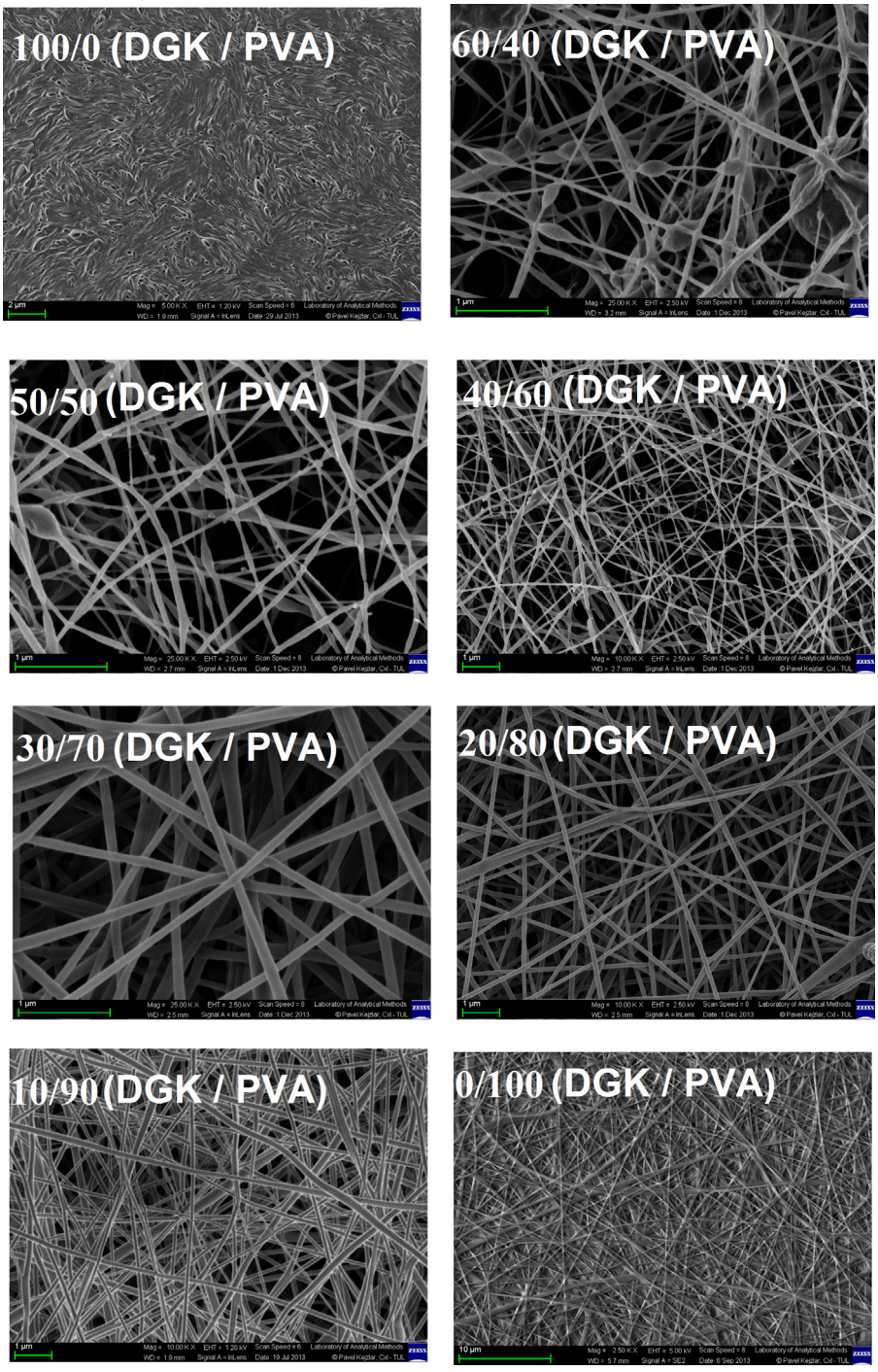

Fig. 1. SEM micrographs of electrospun fibres made from DGK/PVA with various weight ratios (100/0; 60/40; 50/50; 40/60; 30/70; 20/80; 10/90 and 0/100).

O—H stretching vibration of hydrogen bonded hydroxyl groups and asymmetric and symmetric stretching vibrations of C—H band form —CH_2 groups. The absorbance peaks at 1724 cm^{-1} and 1255 cm^{-1} are indicative of acetyl groups present in GK. The peaks at 1610 cm^{-1} and 1429 cm^{-1} present in GK and DGK are due to carboxylate groups of uronic acid residues. The absence of peaks at 1724 cm^{-1} and 1255 cm^{-1} in the ATR-FTIR spectrum in Fig. 4A shows that deacetylation of GK with NaOH was complete. The peaks at 1050 cm^{-1} are assigned to the stretching vibration of the C—O bond (Vinod et al., 2008b). The spectra of PVA indicated at 3350 cm^{-1} (—OH), 2925 cm^{-1} and 2854 cm^{-1} represent asymmetric and symmetric stretching of C—H and —CH_2 groups. The peaks at 1730 cm^{-1} and 1630 cm^{-1} are also attributed to C=O stretching vibrations of carbonate and C—H bending, respectively (Ranjbar-Mohammadi et al., 2013).

The appearance of a peak at 1565 cm^{-1} in the P-NFM represents the deformation vibration of the OH group with an H-bond. This suggests that a hydrogen bond forms between —OH groups of PVA and —COO^- or —OH groups of GK to form PVA/DGK blend in P-NFM (Fig. 4A). Furthermore, the FTIR spectra of P-NFM showed the characteristic peak at 1610 cm^{-1} which corresponds to an asymmetric stretching of carboxylate groups. The peak at 1610 cm^{-1}, for GK shifted to a lower frequency in the P-NFM spectrum and appeared at 1565 cm^{-1}, which indicated that the —COO^- groups

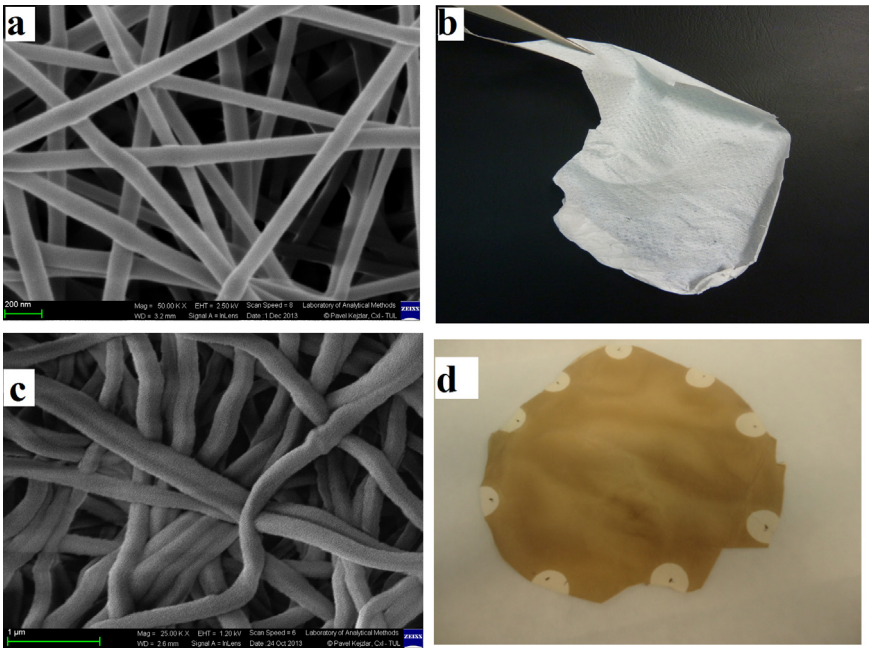

Fig. 2. SEM pictures (a and c) and digital photographs of (b and d) electrospun NFM (70/30) and P-NFM (plasma treated).

are also responsible for the formation of the PVA/DGK blend in NFM. Similar observations have been reported in the case of gum Tragacanth and chitosan with PVA nanofibre formation and the formation of hydrogen bonding between —OH groups of PVA and —COO and —OH groups of gum Tragacanth and chitosan, respectively (Ranjbar-Mohammadi et al., 2013; Jia et al., 2007).

There are still a considerable amount of carboxyl groups left in the P-NFM after heat treatment and methane plasma treatment, which are available for the complexation of nanoparticles with P-NFM. The asymmetric and symmetric stretching vibration of $-COO^-$ from carboxylate group at 1565 cm^{-1} and 1429 cm^{-1} observed in P-NFM, which is shifted to 1620 cm^{-1} in the spectrum of Ag-P-NFM, Au-P-NFM and Pt-P-NFM (Fig. 4B), seems to be the possible interaction between these nanoparticles and carboxylate groups of P-NFM. In addition, the predominant peak observed at 1242 cm^{-1} in Ag P-NFM, Au P-NFM and Pt P-NFM are indicating the interaction between the —C—O groups present in the P-NFM and the nanoparticles, forming complexes with the —C—O groups and nanoparticles (Ag, Au, and Pt). The FTIR spectrum clearly indicates that the carboxylate, carbonyl and hydroxyl groups present in the P-NFM are responsible for the extraction of the nanoparticles (Ag, Au and Pt) from the water. The increased adsorption capacity of P-NFM compared to NFM (Table 3) was suggested due to the additional functional groups created by the plasma treatment.

The adsorption efficiency (AE) determined by Eq. (2) is presented in Table 2. From Table 2 it can be observed that P-NFM have a stronger affinity towards Ag, Au and Pt nanoparticle compared to NFM and the adsorption efficiency decreases in the order Pt > Au > Ag. Adsorption of nanoparticle onto the surface of the membranes can be explained by the interaction between the nanoparticle and the surface functional group of the membrane. DGK has an abundant number of functional groups, such as —OH, —COO and C=O groups, which can interact with nanoparticle and effectively remove them from water. The higher removal efficiency of Pt nanoparticle may be due to their smaller size and therefore larger surface area. These observations are similar to previously reported works on the toxic metal adsorption of GK (Vinod et al., 2010).

The adsorption capacity of the NFM and P-NFM was calculated from the adsorption efficiencies and is presented in Table 3. From Table 3 it can be observed that the Q_e value for Pt is 327.2 mg/g on P-NFM. The Q_e value for Ag and Au was found to be 168.5 mg/g and 320.5 mg/g, respectively. The untreated nanofibres (NFM) have values for Pt, Ag and Au of 270.4 mg/g, 143.4 mg/g

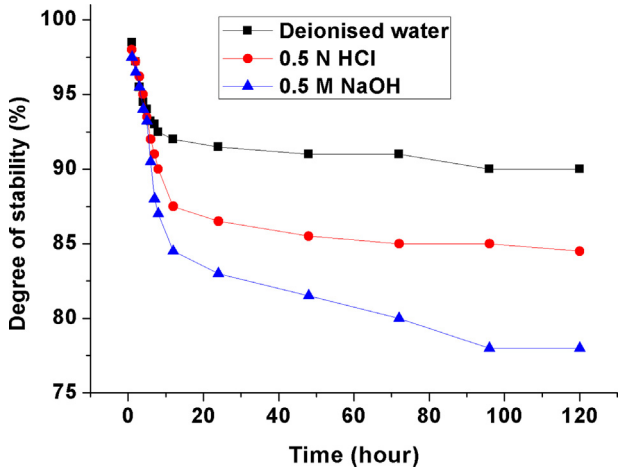

Fig. 3. The degree of stability, DS (%) of P-NFM in deionized water, 0.5N HCl and NaOH after 5 days of contact.

Table 2
Adsorption efficiency (% AE) of nanoparticles (Ag, Au and Pt) on NFM and P-NFM (**Conditions**: Initial nanoparticle concentration in water 2×10^{-4} M; pH 7.0; agitation time 6 h.; agitation speed 200 rpm; temperature 25 °C).

Nanoparticles	Adsorption efficiency, AE (%)	
	P-NFM	NFM
Ag	78.1 ± 1.23	66.5 ± 0.95
Au	81.4 ± 1.05	56.0 ± 0.68
Pt	83.9 ± 1.58	69.3 ± 0.55

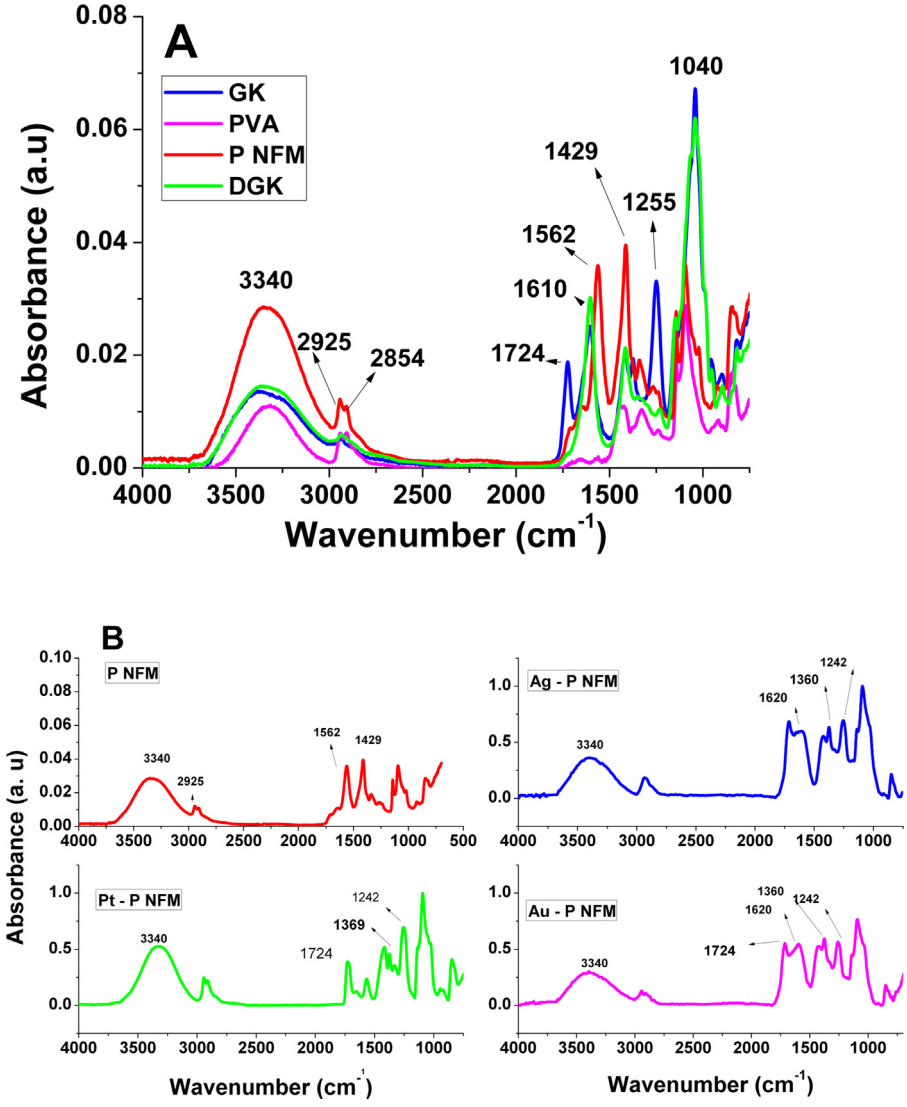

Fig. 4. The ATR-FTIR spectra of GK, DGK, PVA, and P-NFM and the corresponding Ag, Au and Pt adsorbed P-NFM, indicating the evlovment of functional groups of NFM for the adsorption of nanoparticles.

and 173.5 mg/g, respectively. The adsorption capacity varies in the order Pt > Au > Ag, for both P-NFM and NFM, indicating that the size of the nanoparticle influences the adsorption capacity of the NFM. These results are in good agreement with the BET surface area analysis data of the NFM, indicating that the higher surface area of the plasma treated membrane (9.79 m^2/g) leads to a higher extraction efficiency compared to untreated membranes (6.15 m^2/g). These results are in agreement with earlier research works on functionalized electrospun PVA membranes and metal oxides which were used for extraction of NP from water (Mallampati & Valiyaveettil, 2013).

The pseudo-first order and pseudo-second order kinetic equations were used to analyse the kinetic experimental data for the extraction of nanoparticle from water on both membranes. The resulting rate constants are presented in Table 3. The experimental results did not fit the 1st order Lagergren model because the

Table 3
Adsorption capacity Q_e and pseudo-first order and pseudo-second order kinetic parameters for removal of nanoparticle with P-NFM and NFM (**Conditions**: Initial nanoparticle concentration in water 2×10^{-4} M; pH 7.0; agitation time 6 h; agitation speed 200 rpm; temperature 25 °C).

Nanofibre membrane	Nano-particle	EXP	Pseudo-first order kinetic model			Pseudo-second order kinetic model		
		Q_e (mg/g)	q_e (mg/g)	k_1 (1/min)	R^2	q_e (mg/g)	k_2 (g/mg/min)	R^2
P-NFM	Ag	168.5	169.95	0.0194	0.95	166.6	0.0009	0.99
	Au	320.5	272.95	0.0267	0.95	319.4	0.0011	0.99
	Pt	327.2	296.75	0.0302	0.95	325.7	0.0001	0.99
NFM	Ag	143.4	96.39	0.0193	0.98	143.0	0.0029	0.99
	Au	173.5	116.30	0.0145	0.94	174.2	0.0010	0.99
	Pt	270.4	192.58	0.0183	0.87	269.5	0.0008	0.99

q_e values do not agree with the calculated value and correlation coefficients (R^2) are relatively low (Table 3). The correlation coefficients (R^2) for the 2nd order kinetics were >0.99 in all cases. The theoretical q_e values agree perfectly with the experimental Q_e values. This suggests that the adsorption followed a pseudo-second order model (Supporting information 4), which is in agreement with other previously reported adsorption studies (Ho & McKay, 1999).

The adsorption of the nanoparticle on the surface of the P-NFM was confirmed by the use of a scanning electron microscope. The SEM image showed the presence of Ag, Au and Pt nanoparticle on the surface of the membrane (Supporting information 5). The corresponding nanoparticle peaks were also confirmed by EDX analysis (Supporting information 5). SEM analysis indicates that the adsorption of the NP on the surface of the NFM was spread uniformly without any aggregation of NP on the surface of the NFM.

3.5. Desorption and regeneration studies of P-NFM

In order to improve the efficiency of the extraction process and apply the recovery of nanoparticle using NFM in practice, it is necessary to regenerate the adsorbent. P-NFM was subjected to successive adsorption and desorption cycles in order to determine its suitability and stability as an adsorbent. Four cycles of nanoparticles (Ag, Au and Pt) desorption (%) with 0.2 N HCl as the desorbing agent are presented (Supporting information 6).

The adsorption/desorption and regeneration were successful for a total of five cycles with the removal and recovery of nanoparticle decreasing only slightly. A small fraction of nanoparticle adsorbed by P-NFM was not recoverable by regeneration using 0.2N HCl because of a strong interaction of the surface functional group with the nanoparticle. The results indicate that P-NFM can be used repeatedly for up to five adsorption/desorption cycles without any damage to the membrane.

3.6. Comparison of nanoparticles removal with different electrospun NFM

The adsorption capacities of the studied nanofibre membranes for the removal of nanoparticles were compared with those reported in the literature (Table 4). The extraction capacity of P-NFM for nanoparticle is comparable to that of the majority of the nanofibres reported in the literature. The adsorption capacity of the NFM and P-NFM are observed to be much higher towards the removal of nanoparticles compared to the other adsorbents used in the contemporary literature (Table 4). The NFM and P-NFM were successively used for the removal of nanoparticles such as Ag, Au and Pt from water. Pt nanoparticles with the smallest size (2.4 ± 0.7 nm) has a higher adsorption capacity (270.4 mg/g and 327.2 mg/g, respectively) compared to Au and Ag nanoparticles with particle sizes 7.8 ± 2.3 nm and 10.5 ± 3.5 nm onto nanofibre membrane (NFM) and methane plasma treated membrane (P-NFM). Even though the adsorption capacity of nanoparticles onto NFM and P-NFM was found higher, however, the adsorption equilibrium time of membranes (NFM and P-NFM) are slightly higher (6 h) than the values for the extraction of nanoparticles (3–6 h) reported in the literature. Nevertheless, the desorption and the reusability of the P-NFM for the four cycles of operation are found to be excellent compared to surface modified electrospun poly(vinyl alcohol) membranes which were used for the extraction of nanoparticles from water (Mahanta & Valiyaveettil, 2011). The high adsorption capacity of the P-NFM might be due to the high surface area, remarkable stability of NFM and P-NFM in acidic, alkali and neutral solutions, modified surface properties and formation of additional functional groups due to plasma treatment. Furthermore the superior properties of the GK such as non-toxicity, biocompatibility, biodegradability and a large number of surface functional groups in its structure are the merits of this gum compared to other synthetic materials used for the removal of the nanoparticles and other toxic pollutants from contaminated water. Therefore, we can

Table 4
Comparison of the extraction performance of P-NFM and NFM with material used for the removal of nanoparticles and heavy metals from water reported in the literature.

Material used	Nanoparticles	Adsorption capacity (mg/g)	Ref.
PVA-MSA	Au	83.27	Mahanta & Valiyaveettil, 2011
	Ag	23.83	
PVA-MPA	Au	79.13	Mahanta & Valiyaveettil, 2011
	Ag	23.95	
PVA-LYS	Au	84.63	Mahanta & Valiyaveettil, 2011
	Ag	55.8	
Metal oxides			
NiO	Ag	54.84	Mallampati & Valiyaveettil, 2013
	Au	76.8	
CeO	Ag	51.04	
	Au	48.94	Mallampati & Valiyaveettil, 2013
ZnO	Ag	47.56	
	Au	45.84	
Co_3O_4	Ag	41.89	Mallampati & Valiyaveettil, 2013
	Au	32.27	
CuO	Ag	5.02	
	Au	3.38	
Polyacrylonitrile/polypyrrole core/shell nanofibre mat	Cr(VI)	74.91	Wang, Pan, He, and Cao (2013)
Poly(acrylo-amidino ethylene amine) nanofibre membrane	As(V)	76.92	Vu, Li, and Ce (2013)
Amine functionalized block copolymers	Ag	99–117	Qureshi et al. (2014)
	Au	50–109	
P-NFM	Ag	168.5	Present study
	Au	320.5	
	Pt	327.2	
NFM (untreated)	Ag	143.4	Present study
	Au	173.5	
	Pt	270.4	

state that plasma treated P-NFM has a significant potential for the removal of nanoparticles from aqueous solutions.

4. Conclusions

Plasma treated electrospun nanofibre membranes based on natural hydrocolloid GK, blended with PVA were utilized to remove nanoparticles from water. Adsorption analysis indicates that Pt nanoparticles show the highest adsorption capacity on P-NFM compared to other nanoparticles (Ag and Au) used in the present study. Furthermore, P-NFM was found to be a very efficient material due to its high surface properties, increase in surface roughness and additional functional group formation after plasma treatment, which was assessed by SEM, BET and FTIR analysis. The adsorption kinetic study suggests that the pseudo-second order kinetic model was suitable to explain the nature of the adsorption of nanoparticles onto NFM. Moreover, plasma treated electrospun membranes were applied for the extraction of nanoparticles from an aqueous environment. These newly synthesized plasma treated membranes show a great potential for the development of environmentally friendly materials for the removal of pollutants from water.

Acknowledgements

The research presented in this article was supported by the Ministry of Education, Youth and Sports (grant no. LO1201) in the framework of the targeted support of the "National Programme for Sustainability I" LO 1201, the OPR&DI project "Centre for Nanomaterials, Advanced Technologies and Innovation", CZ.1.05/2.1.00/01.0005.

References

Choi, K.-J., Kim, S.-G., & Kim, S.-H. (2008). Removal of antibiotics by coagulation and granular activated carbon filtration. *Journal of Hazardous Materials*, *151*, 38–43.
Desai, K., Kit, K., Li, J. J., Davidson, P. M., Zivanovic, S., & Meyer, H. (2009). Nanofibrous chitosan non-wovens for filtration applications. *Polymer*, *50*, 3661–3669.
Fang, X., Xiao, S., Shen, M., Guo, R., Wang, S., & Shi, X. (2011). Fabrication and characterization of water-stable elecrospun polyethyleneimine/polyvinyl alcohol nanofibers with super dye sorption capability. *New Journal of Chemistry*, *35*, 360–368.
Frenot, A., & Chronakis, I. S. (2003). Polymer nanofibers assembled by electrospinning. *Current Opinion in Colloid and Interface Science*, *8*, 64–75.
Garcia, N., Moreno, J., Cartmell, E., Rodriguez-Roda, J., & Judd, S. (2013). The application of microfiltration-reverse osmosis/nanofiltration to trace organics removal for municipal wastewater reuse. *Environmental Technology*, *34*(24), 1–7.
Guo, M., Ding, B., Li, X. H., Wang, X. L., Yu, J. Y., & Wang, M. R. (2010). Amphiphobic nanofibrous silica mats with flexible and high-heat-resistant properties. *Journal of Physical Chemistry C*, *114*, 916–921.
Ho, Y. S., & McKay, G. (1999). Comparative of chemisorptions kinetics models applied to pollutant removal on various sorbents. *Journal of Environmental Science and Health Perspective A*, *34*, 1179–1204.
Homayoni, H., Ravandi, S. A. H., & Valizadeh, M. (2009). Electrospinning of chitosan nanofibers: Processing optimization. *Carbohydrate Polymers*, *77*, 656–661.
Kim, H. S. K., Kim, K. H. J., Jin, H. J., & Chin I.J., I. J. (2005). Morphological characterization of electrospun nano-fibrous membranes of biodegradable poly(L-lactide) and poly(lactide-*co*-glycolide. *Macromolecular Symposia*, *224*, 145–154.
Kovalova, L., Siegrist, H., Von Gunten, U., Eugster, J., Hagenbuch, M., Wittmer, A., et al. (2013). Elimination of micro pollutants during post-treatment of hospital wastewater with powdered activated carbon, ozone, and UV. *Environmental Science and Technology*, *47*, 7899–7908.
Lee, K. H., Kim, H. Y., Bang, H. J., Jung, Y. H., & Lee, S. G. (2003). The change of bead morphology formed on electrospun polystyrene fibers. *Polymer*, *44*, 4029–4034.
Le Cerf, D., Irinei, F., & Muller, G. (1990). Solution properties of gum exudates from *Sterculia urens* (karaya gum). *Carbohydrate Polymers*, *13*, 375–386.
Li, S., Yue, X., Jing, Y., Bai, S., & Dai, Z. (2011). Fabrication of zonal thiol-functionalized silica nanofibers for removal of heavy metal ions from wastewater. *Colloids and Surfaces A: Physicochemical and Engineering Aspects*, *380*, 229–233.
Luo, Y., Guo, W., Ngo, H. H., Nghiem, L. D., & Hai, F. I. (2014). A review on the occurrence of micropollutants in the aquatic environment and their fate and removal during waste water treatment. *Science for Total Environment*, *473–374*, 619–641.
Jia, Y.-T., Gong, J., Gu, X.-H., Kim, H.-Y., Dong, J., & Sen, X.-Y. (2007). Fabrication and characterization of poly(vinyl alcohol)/chitosan blend nanofibers produced by electrospinning method. *Carbohydrate Polymers*, *67*, 403–409.
Mahanta, N., & Valiyaveettil, S. (2011). Surface modified electrospun poly(vinyl alcohol) membranes for extracting nanoparticles from water. *Nanoscale*, *3*, 4625–4631.
Mahendran, T., Williams, P. A., Phillips, G. O., Al-Assaf, S., & Baldwin, T. C. (2008). New insights into the structural characteristics of the arabinogalactan-protein (AGP) fraction of gum Arabic. *Journal of Agricultural and Food Chemistry*, *56*, 9269–9276.
Mallampati, R., & Valiyaveettil, S. (2013). Biomimetic metal oxides for the extraction of nanoparticles from water. *Nanoscale*, *5*, 3395–3399.
Muzzarelli, R. A. A., Mehtedi M., E. I., & Mattioli-Belmonte, M. (2014). Emerging biomedical applications of nano-chitins and nano-chitosans obtained via advanced eco-friendly technologies from marine resources. *Marine Drugs*, *12*, 5468–5502.
Ranjbar-Mohammadi, M., Bahrami, S. H., & Joghataei, M. T. (2013). Fabrication of novel nanofibre scaffolds from gum tragacanth/poly(vinyl alcohol) for wound dressing application: In vitro evaluation and antibacterial properties. *Materials Science and Engineering C*, *33*, 4935–4943.
Naidu, V. G. M., Madhusudhana, K., Sashidhar, R. B., Ramakrishna, S., Khar, R. K., Ahmed, F. J., et al. (2009). Polyelectrolyte complexes of gum kondagogu and chitosan, as diclofenac carriers. *Carbohydrate Polymers*, *76*, 464–471.
Naidu, V. G. M., Ramakrishna, S., Palaniappan, S., Sashidhar, R. B., Khar, R. K., & Diwan, P. V. (2009). Emulsifying properties of gum kondagogu (*Cochlospermum gossypium*), a natural biopolymer. *Journal of Science and Food Agriculture*, *89*, 1271–1276.
Phillips, G. O., & Williams, P. A. (2001). Tree exudates gums: Natural and versatile food additives and ingredients. *Food Ingredients and Analytical International*, *23*, 26–28.
Qureshi, Z. S. R., DSouza, R., Mallampati, R., & Valiyaveettil, S. (2014). Synthesis of amine functionalized block copolymers for nanopollutant removal from water. *Journal of Applied Polymer Science*,, *2014* http://dx.doi.org/10.1002/APP.40943
Radjenovic, J., Petrovic, M., & Barcelo, D. (2009). Fate and distribution of pharmaceuticals in waste-water and sewage sludge of the conventional activated sludge (CAS) and advanced membrane bioreactor (MBR) treatment. *Water Research*, *43*, 831–841.
Schafer, A. I., Nghiem, L. D., & Semiao, A. J. C. (2011). Micropollutant sorption to membrane polymers: A review of mechanisms for estrogens. *Advanced Colloid Interface*, *164*, 100–117.
Still, T. J., & Von Recum, H. A. (2008). Electrospinning: Applications in drug delivery and tissue engineering. *Biomaterials*, *29*, 1989–2006.
Suarez, S., lema, J. M., & Omil, F. (2009). Pre-treatment of hospital wastewater by coagulation-flocculation and flotation. *Bioresource Technology*, *100*, 2138–2146.
Svirachev, D. M., & Tabaliov, N. A. (2005). Plasma treatment of polymer surfaces in different gases. *Bulgarian Journal of Physics*, *32*, 22–33, 2005.
Thanasi, V., Singh, G., & Ramakrishna, S. (2008). Electrospun nanofibres in energy and environmental applications. *Energy and Environmental Science*, *1*, 205–221.
Toskas, G., Hund, R.-D., Laourine, E., Cherif, C., Smyrniotopoulos, V., & Roussis, V. (2011). Nanofibers based on polysaccharides from the green seaweed Ulva Rigida. *Carbohydrate Polymers*, *84*, 1093–1102.
Verbeken, D., Dierckx, S., & Dewettinck, K. (2003). Exudate gums: Occurrence, production, and applications. *Applied Microbiology and Biotechnology*, *63*, 10–21.
Vinod, V. T. P., Sashidhar, R. B., & Sukumar, A. A. (2010). Competitive adsorption of toxic heavy metal contaminants by gum kondagogu (*Cochlospermum gossypium*): A natural hydrocolloid. *Colloids and Surface B: Biointerfaces*, *75*, 490–495.
Vinod, V. T. P., Sashidhar, R. B., Suresh, K. I., Rama Rao, B., Vijaya Saradhi, U. V. R., & Prabhakar Rao, T. (2008). Morphological, physico-chemical and structural characterization of gum kondagogu (*Cochlospermum gossypium*): A tree gum from India. *Food Hydrocolloids*, *22*, 899–915.
Vinod, V. T. P., Sashidhar, R. B., Sarma, V. U., & Vijay Saradhi, U. V. (2008). Compositional analysis and rheological properties of gum kondagogu (cochlospermum gossypium): A tree gum from India. *Journal of Agricultural and Food Chemistry*, *56*, 2199–2207.
Vinod, V. T. P., & Sashidhar, R. B. (2009). Solution and conformational properties of gum kondagogu (*Cochlospermum gossypium*): A natural product with immense potential as a food additive. *Food Chemistry*, *116*, 686–692.
Vinod, V. T. P., Saravanan, P., Sreedhar, B., Keerthi Devi, D., & Sashidhar, R. B. (2011). A facile synthesis and characterization of Ag, Au and Pt nanoparticles using a natural hydrocolloid gum kondagogu (*Cochlospermum gossypium*). *Colloids and Surfaces B: Biointerfaces*, *83*, 291–298.
Vinod, V. T. P., Sashidhar, R. B., Sreedhar, B., Rama Rao, B., Nageswara Rao, T., & Johny, T. A. (2009). Interaction of Pb^{2+} and Cd^{2+} with gum kondagogu (*Cochlospermum gossypium*): A natural carbohydrate polymer with biosorbent properties. *Carbohydrate Polymers*, *78*, 894–901.
Vu, D., Li, X., & Ce, W. (2013). Efficient adsorption of As (V) on poly(acrylo-amidino ethylene amine) nanofiber membranes. *Chinese Science Bulletin*, *58*, 1702–1707.
Wang, X., Ding, B., Yu, J., & Wang, M. (2011). Engineering biomimetric superhydrophobic surfaces of electrospun nanomaterials. *Nano Today*, *6*, 510–530.
Wang, J., Pan, K., He, Q., & Cao, B. (2013). Polyacrylonitril/polypyrrole core/shell nanofiber mat for the removal of hexavalent chromium from aqueous solution. *Journal of Hazardous Materials*, *244–245*, 121–129.
Wilkes, G.L. available from: http://www.che.vt.edu/Wilkes/electrospinning/electrospinning.html. 2001.
Yangali-Quintanilla, V., Maeng, S. K., Fujioka, T., Kennedy, M., Li, Z., & Amy, G. (2011). Nano filtration vs. reverse osmosis for the removal of emerging organic contaminants in water reuse. *Desalination and Water Treatment*, *34*, 50–56.